

SCIENTIFIC REPORTS



OPEN

Direct synthesis of hydrogen peroxide from plasma-water interactions

Jiandi Liu¹, Bangbang He², Qiang Chen², Junshuai Li³, Qing Xiong⁴, Guanghui Yue⁵, Xianhui Zhang², Size Yang², Hai Liu² & Qing Huo Liu⁶

Received: 27 June 2016
Accepted: 09 November 2016
Published: 05 December 2016

Hydrogen peroxide (H₂O₂) is usually considered to be an important reagent in green chemistry since water is the only by-product in H₂O₂ involved oxidation reactions. Early studies show that direct synthesis of H₂O₂ by plasma-water interactions is possible, while the factors affecting the H₂O₂ production in this method remain unclear. Herein, we present a study on the H₂O₂ synthesis by atmospheric pressure plasma-water interactions. The results indicate that the most important factors for the H₂O₂ production are the processes taking place at the plasma-water interface, including sputtering, electric field induced hydrated ion emission, and evaporation. The H₂O₂ production rate reaches ~1200 μmol/h when the liquid cathode is purified water or an aqueous solution of NaCl with an initial conductivity of 10500 μS cm⁻¹.

Hydrogen peroxide (H₂O₂) has found many applications in modern industry including acting as a strong oxidizer, a bleaching agent, disinfectant, and the propellant in rocketry^{1,2} etc. due to the specific property of its oxygen-oxygen single bond. At present, the industrial production of H₂O₂ is dominated by the anthraquinone process which needs multistep processes and consumes much energy³. Therefore, a direct synthesis of H₂O₂ is required to avoid the disadvantages of anthraquinone process. Obviously, H₂O₂ synthesis directly from its constituent elements, i.e., H₂ and O₂, is a simple idea⁴⁻⁶, but the mixture of H₂ and O₂ is explosive. Some alternative direct methods do not use H₂ and O₂ which avoid the explosive problem and enable the *in-situ* continuous synthesis of H₂O₂, such as electrochemical synthesis from O₂ and water⁷⁻¹¹, photocatalytic TiO₂ in aqueous solutions¹²⁻¹⁵, and even sunlight-driven production from water and O₂ although the production rate is relatively low (0.625 μmol/h)¹⁶.

It has been proven that H₂O₂ can be formed by the reaction of H₂ + O₂ → H₂O₂ in plasma containing H₂ and O₂ gases¹⁷⁻¹⁹. When plasma is in contact with water, the plasma-water interactions can entail many direct reactions at the plasma-water interface and indirect cascade reactions in the bulk water²⁰⁻²⁵. One important species at the plasma-water interface is hydroxyl radical (OH) produced by plasma-induced water reactions with electrons and ions. The exact OH formation pathways by plasma-water interactions are very complicated, and one can refer to a review paper²⁶ for details. As the building blocks, the generated OH radicals combination contributes to the main process of H₂O₂ formation in plasma-water interactions. In addition, other less probable pathways such as OH + H₂O⁺ → H₂O₂ + H^{27,28} are also possible. In fact, there exist many reports on the H₂O₂ formation by discharge plasma operated over and inside aqueous solutions²⁷⁻³⁵. However, the determining factors which influence the H₂O₂ production from the plasma-water interactions remain unclear. To optimize the H₂O₂ production from plasma-water interactions, a better understanding of the H₂O₂ production process is desired. Herein, we present an insight into

¹Institute of Electromagnetics and Acoustics, Department of Materials Science and Engineering, College of Materials, Xiamen University, Xiamen 361005, China. ²Fujian Provincial Key Laboratory of Plasma and Magnetic Resonance, Institute of Electromagnetics and Acoustics, Department of Electronic Science, Xiamen University, Xiamen 361005, China. ³Key Laboratory of Special Function Materials & Structure Design of the Ministry of Education, Key Laboratory for Magnetism & Magnetic Materials of the Ministry of Education, and School of Physical Science & Technology, Lanzhou University, 222 South Tianshui Road, Lanzhou 730000, China. ⁴State Key Laboratory of Power Transmission Equipment & System Security and New Technology, Chongqing University, Chongqing 400044, China. ⁵Department of Materials Science and Engineering, College of materials, Xiamen University, Xiamen 361005, China. ⁶Department of Electrical and Computer Engineering, Duke University, Durham, NC 27708, USA. Correspondence and requests for materials should be addressed to Q.C. (email: chenqiang@xmu.edu.cn) or H.L. (email: liuhai8619@xmu.edu.cn)

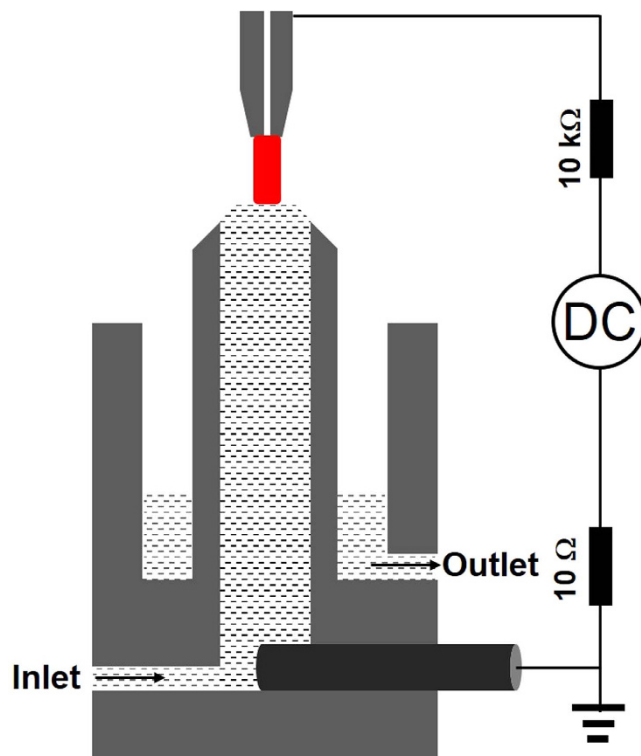


Figure 1. Schematic diagram of the device for the H_2O_2 production.

the understanding of H_2O_2 production by the plasma-water interactions. The results indicate that the sputtering, the electric field induced ion emission, and the evaporation at the water surface strongly influences the H_2O_2 production.

Results

Experimental approach and the H_2O_2 production. H_2O_2 was produced by the device schematically shown in Fig. 1 [see Supplementary Information (SI) for details]. A direct current Ar atmospheric pressure plasma was generated between a tungsten steel tube (1.02 mm and 6.35 mm in inner and outside diameters, respectively) and a liquid surface. The liquid acts as cathode or anode (positive or negative voltage applied to the tungsten steel electrode), and NaCl was used to adjust the initial conductivity of the liquid. The Ar flow rate, the discharge current, and the gap between the tungsten steel tube and the liquid surface were set to be 20 sccm, 30 mA, and 3 mm, respectively. To refresh the surface liquid, the total 400 ml liquid was circulated by a peristaltic pump at a flow rate of 200 ml/min. During the plasma-solution interactions, the H_2O_2 yield was measured at a given interval of 10 min, and the temperature, pH value, and the conductivity of the solution were also investigated.

Figure 2 presents the H_2O_2 yields at different experimental conditions. For liquids with low initial conductivities ($1.60 \mu\text{S cm}^{-1}$ and $1440 \mu\text{S cm}^{-1}$), the H_2O_2 production rate (the slope of the yield curve) decreases with increasing time, while they are constants for the liquids with high initial conductivities ($4800 \mu\text{S cm}^{-1}$ and $10500 \mu\text{S cm}^{-1}$) [Fig. 1(a)]. Even with an initial conductivity of $4800 \mu\text{S cm}^{-1}$, the H_2O_2 yield for NaOH solution is almost zero after 60 min plasma treatment [Fig. 1(b)]. As the discharge current increases, the H_2O_2 production rate is enhanced [Fig. 1(c)]. When the liquid acts as anode (negative voltage applied to the tungsten steel electrode), there is almost no H_2O_2 production [Fig. 1(d)]. These results guide us to a question: What is the underlying mechanism for these differences? To answer this question, we must carefully analyse the processes taking place at the plasma-liquid interfaces from which the H_2O_2 is formed during the plasma-liquid interactions.

Water molecule transfer processes at the plasma-liquid interface. When the liquid acts as cathode, a cathode voltage fall (V_C) will be built between the plasma and the liquid surface due to the space charge accumulation^{36–40}. The V_C will be located at a limited distance called cathode sheath, and for an atmospheric pressure discharge plasma, the thickness of the cathode sheath is smaller than $100 \mu\text{m}$ when the discharge current is more than 5 mA ³⁶. In our case, the discharge current is 30 mA, it is reasonable to take the sheath thickness as $100 \mu\text{m}$. Table 1 presents the V_C for liquids with different initial conductivities (see SI for the details of the V_C estimation). The following analysis will demonstrate that this cathode region near the liquid surface is very important to the water molecules transfer at the plasma-liquid interface.

Figure 3 depicts three processes contributing to the water transfer from the liquid phase to the gaseous plasma, and the qualitative characteristics of the voltage potential (V) and the electric field (E) in the plasma-liquid system (ref. 41). Firstly, positive ions in the plasma passing the cathode sheath will be accelerated by the V_C and the constituents of liquid will be sputtered into the gaseous phase by the accelerated energetic ions. This sputtering process has been widely used in low pressure plasma for material fabrication⁴¹. Secondly, the V_C measured in our

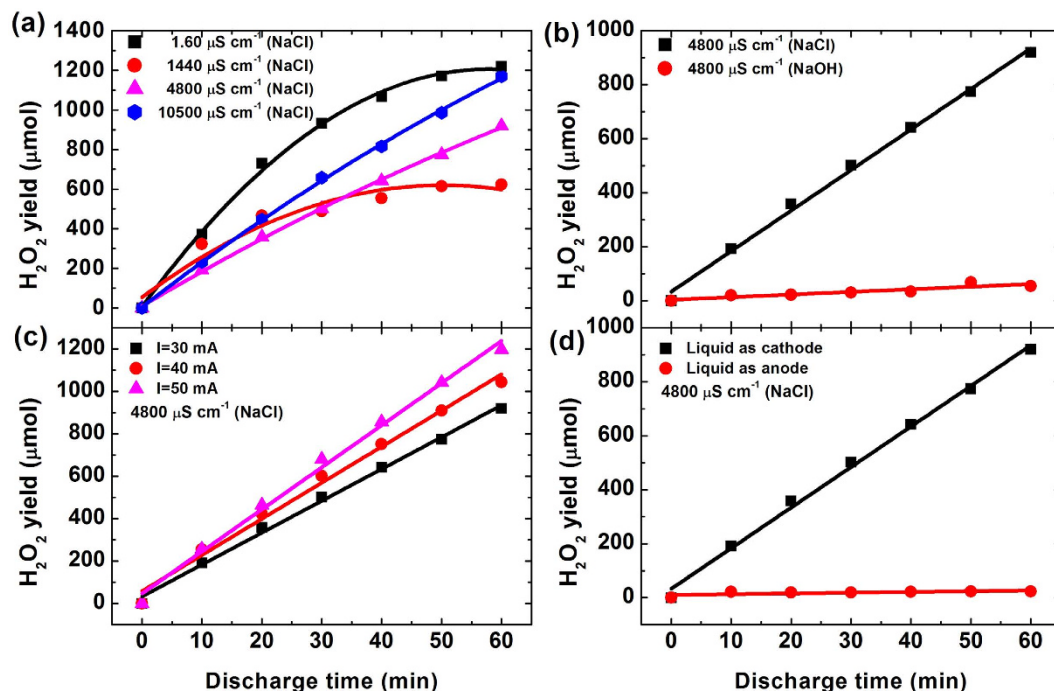


Figure 2. H_2O_2 yields at different experimental conditions. Plasma-liquid interactions were performed with liquids of (a) initial conductivities of 1.60, 1440, 4800 and $10500 \mu\text{S cm}^{-1}$, (b) NaCl and NaOH with the same initial conductivity of $4800 \mu\text{S cm}^{-1}$, (c) NaCl with the initial conductivity of $4800 \mu\text{S cm}^{-1}$ at discharge currents of 30 mA, 40 mA and 50 mA, and (d) NaCl with an initial conductivity of $4800 \mu\text{S cm}^{-1}$ (The liquid acts as cathode or anode).

Time (min)	V_c (V)			
	$1.60 \mu\text{S cm}^{-1}$	$1440 \mu\text{S cm}^{-1}$	$4800 \mu\text{S cm}^{-1}$	$10500 \mu\text{S cm}^{-1}$
0	N/A ^[a]	581	504	512
20	663	559	494	505
40	590	544	507	510
60	558	526	493	506

Table 1. Cathode voltage falls (V_c) for liquids with different initial conductivities. NaCl was used to adjust the solution conductivity. [a] Data are unavailable because the discharge is unstable in the very beginning for the liquid with an initial conductivity of $1.60 \mu\text{S cm}^{-1}$.

case is in the magnitude of $\sim 500 \text{ V}$ (see Table 1) which forms an electric field in the order of 100 kV cm^{-1} near the liquid surface (see latter analysis for the electric field estimation). This electric field is high enough to pull out the hydrated negative ions (carrying water molecules) from the liquid surface and transfer them to the gaseous plasma^{36,42–44}, which is similar to the field emission at a solid surface. Thirdly, there is evaporation at the liquid surface caused by plasma and Joule heating. Obviously, all these three processes can transfer water molecules from the liquid phase into the gaseous plasma, and then the number of water molecules entering the plasma phase is influenced by the above three processes. Water molecules in the gaseous plasma can react with plasma species to form OH, and then H_2O_2 is formed by the combination of OH. Finally, H_2O_2 dissolves into the liquid to form an aqueous solution. Therefore, H_2O_2 production will increase with the number of water molecules entering the plasma phase which is strongly dependent on the above mentioned processes.

The number density of water molecules (n) entering the plasma phase can be expressed as

$$n = n_{\text{Spu}} + n_{\text{Ele}} + n_{\text{Eva}} \quad (1)$$

where

n_{Spu} : the number density of water molecules entering the plasma phase due to the sputtering, n_{Spu} is related to the cathode voltage fall (V_c), discharge current (I_d), liquid surface tension etc. and it can be described as $n_{\text{Spu}} = k_{\text{Spu}} I_d (E_i)^{1/241}$, k_{Spu} is the sputtering coefficient, and E_i is the energy of incident ion. The positive ion in the plasma obtains its energy by passing the plasma cathode sheath, and therefore the obtained energy is proportional to the V_c . Thus, n_{Spu} can be expressed as $n_{\text{Spu}} = k_{\text{Spu}} I_d (V_c)^{1/2}$.

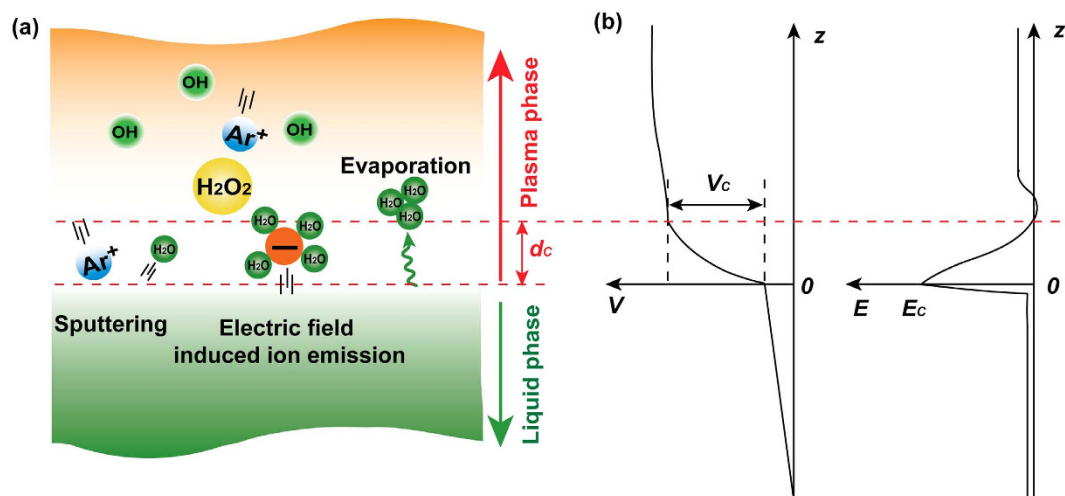


Figure 3. Characteristics of the plasma-liquid interface. (a) Three main processes occurring at the plasma-liquid interface as the liquid is cathode, and (b) the qualitative characteristics of the voltage potential (V) and electric field (E) in the plasma-liquid system (ref. 41). z is the coordinate along the plasma-liquid direction and at the liquid surface $z = 0$, V_c is the cathode voltage fall, d_c is the thickness of the cathode sheath, and E_c is the electric field at the liquid surface.

Initial conductivities ($\mu\text{S cm}^{-1}$)	Power (10^{-3} kW)	Energy Yield (mg kWh^{-1})	Generation Rate (mg h^{-1})
1.60	38.1	1089	41.48
1440	24.5	866	21.22
4800	23.1	1354	31.28
10500	22.8	1741	39.78

Table 2. Consumed power, energy yield and the generation rate of hydrogen peroxide generation for liquids with different initial conductivities. NaCl was used to adjust the solution conductivity.

n_{Ele} : the number density of water molecules entering the plasma phase due to the electric field induced hydrated ion emission, and n_{Ele} is an increasing function of the ion concentration in the liquid phase (C_{Ion}) and the electric field near the liquid surface (E_c) but depends on these parameters in a complicated way⁴⁴. We can express it as $n_{Ele} = f(V_c, C_{Ion})$. In addition, the electric field near the liquid surface (E_c) can be estimated as follows. In the cathode sheath, $E = E_c(1 - z/d_c)$, and $V = V_c(z/d_c)(2 - z/d_c)$, where E is the electric field in the cathode sheath, z is the distance away from the liquid surface, d_c is the thickness of cathode sheath, V is the voltage potential in the cathode sheath, and V_c is the voltage potential near the liquid surface⁴¹. If we integrate E to get V , we can find that $E_c = 2V_c/d_c$. From the results and analysis in the main paper, we know that the V_c in liquid cathode is in the magnitude of ~ 500 V, and d_c is taken as $100 \mu\text{m}$, and then E_c is estimated to be in the order of 100 kV cm^{-1} .

n_{Eva} : the number density of water molecules entering the plasma phase due to evaporation. Based on the thermodynamics law, n_{Eva} can be expressed as $n_{Eva} = n_0 \exp(-W/kT)$, where n_0 is the number density of water molecules in the liquid phase, W is the heat of evaporation, k is the Boltzmann constant and T is the liquid temperature.

Therefore, n can be expressed as

$$n = k_{Spu} I_d (V_c)^{1/2} + f(V_c, C_{Ion}) + n_0 (-W/kT) \quad (2)$$

Besides depending on I_d for n_{Spu} , and on C_{Ion} for n_{Eva} , both n_{Spu} and n_{Ele} depend on the cathode voltage fall (V_c), and n_{Eva} depends on the solution temperature.

H_2O_2 energy yields. Based on the discharge voltages shown in Fig. S2, we estimated the average power consumed in the plasma-liquid interactions, and then the H_2O_2 generation energy yields were calculated for liquids with different initial conductivities and the results are summarized in Table 2. The H_2O_2 energy yields are larger than most of the H_2O_2 energy yields generated from discharge plasmas which have been summarized in ref. 28. The maximum energy yield appears for liquid with an initial conductivity of $10500 \mu\text{S cm}^{-1}$, although the liquid with an initial conductivity of $1.6 \mu\text{S cm}^{-1}$ produces the largest generation rate. The energy yield can be expressed as

$$\text{Energy yield} = \frac{\text{Generation rate}}{\text{Energy}_{Liq} + \text{Energy}_{Pla-Liq}} \quad (3)$$

where $Energy_{Liq}$ and $Energy_{Pls-Liq}$ are energy consumed in the liquid (mostly taking a form of heating the liquid cylinder) and energy consumed in the plasma-liquid interactions, respectively, and only the latter contributes to the H_2O_2 production. Therefore, $Energy_{Liq}$ can affect the energy yield of the H_2O_2 formation. The largest generation rate for the liquid with an initial conductivity of $1.6\ \mu S\ cm^{-1}$ can be attributed to the high resistance of the liquid cylinder between the plasma and the graphite electrode. The Joule heating consumes a large portion of the supplied power in the liquid with the initial conductivity of $1.6\ \mu S\ cm^{-1}$, but in this case, a larger cathode voltage fall is close to the liquid surface as shown in Table 1, and therefore, it produces a large H_2O_2 generation rate with a lower energy yield if compared with the case using liquid with the initial conductivity of $10500\ \mu S\ cm^{-1}$. In the plasma-induced H_2O_2 generation, to select the liquid with a high or low initial conductivity is dependent on one's aim: to obtain high energy yield or high generation rate.

Discussion

Based on the expression of n , the water molecules transfer from the liquid phase to the gaseous plasma is largely determined by the sputtering and the electric field induced hydrated ion emission in the case of liquid cathode since the evaporation for all cases are estimated to be similar [Fig. S6(a)]. The results in Table 1 indicate that the V_C decreases with increasing time for liquids with initial conductivities of $1.60\ \mu S\ cm^{-1}$ and $1440\ \mu S\ cm^{-1}$, while it almost keeps constant for liquids with initial conductivities of $4800\ \mu S\ cm^{-1}$ and $10500\ \mu S\ cm^{-1}$. Therefore, from the expression of n and the data in Table 1, one can deduce that n for liquids with initial conductivities of $1.60\ \mu S\ cm^{-1}$ and $1440\ \mu S\ cm^{-1}$ will decrease with increasing time, while it is almost constant for the liquids with initial conductivities of $4800\ \mu S\ cm^{-1}$ and $10500\ \mu S\ cm^{-1}$. Therefore, the H_2O_2 production rate decreases as time increases for liquids with low initial conductivity, while it is almost constant for liquids with high initial conductivity. Because the evaporation for all cases are estimated to be similar [see Fig. S6(a)], n is determined by I_d , V_C and C_{Ion} . For the case with a constant I_d , n is related to V_C and C_{Ion} . Although C_{Ion} is low in case of the liquid with low conductivity ($1.6\ \mu S\ cm^{-1}$), n can be still large since the high V_C (see Table 1) in this case. Therefore, there is a high H_2O_2 production rate for the liquid with a low conductivity ($1.6\ \mu S\ cm^{-1}$). In addition, the estimated V_C are almost the same for discharge currents of 30 mA, 40 mA and 50 mA ($\sim 500\ V$, not shown). When the discharge current increases, the ion flux (related to I_d) near the liquid surface is enhanced and thus water transfer from the liquid phase to the gaseous plasma is increased. Consequently, the H_2O_2 yield increases with increasing discharge current as shown in Fig. 2(c). The estimated V_C for NaOH solution with an initial conductivity of $4800\ \mu S\ cm^{-1}$ is $\sim 30\ V$ higher than that for the NaCl solution with the same conductivity. Based on the above analysis, one must expect that the NaOH solution should produce more H_2O_2 . However, the H_2O_2 yield for NaOH solution is almost zero as shown in Fig. 2(b). The reason might be as follows. H_2O_2 is a weak acid and it can react with OH^- to form HO_2^- in concentrated NaOH solution ($H_2O_2 + OH^- \rightarrow HO_2^- + H_2O$)^{45–47}. Therefore, the produced H_2O_2 was consumed by reacting with NaOH, resulting in a very low H_2O_2 yield.

When liquid acts as anode, the cathode voltage fall is formed on the tungsten steel electrode, and therefore there is no sputtering and electric field induced ion emission at the liquid surface, and evaporation is the only way to transfer water molecules from liquid phase into the gaseous plasma. Compared with the case of liquid cathode, n is insignificantly small in the case of liquid anode, resulting in a low H_2O_2 yield as shown in Fig. 2 (b). Comprison of OH optical emission intensity in cases of liquid cathode and anode also confirms this conclusion (Fig. S9).

In summary, using water as the only consumed material, H_2O_2 is directly synthesized by plasma-water interactions and the H_2O_2 production rate can reach $1200\ \mu mol/h$ when the liquid cathode is purified water or NaCl solution with an initial conductivity of $10500\ \mu S\ cm^{-1}$. The H_2O_2 production rate strongly depends on the plasma-liquid interactions at the liquid surface: sputtering, high electric field induced hydrated ion emission, and evaporation. Liquid cathode performs much better than liquid anode in producing H_2O_2 by plasma-water interactions. In addition, the synthesized H_2O_2 can be consumed if the liquid contains some constituent able to react with H_2O_2 such as NaOH.

Methods

Measurement of the H_2O_2 yield. Because H_2O_2 can react with titanium sulfate. in strong acid to form H_2TiO_4 ($Ti^{4+} + H_2O_2 + 2H_2O \rightarrow H_2TiO_4 + 4H^+$) and the absorption intensity of the yellow-coloured H_2TiO_4 in 410 nm is proportional to the reacted H_2O_2 concentration^{15,48–50}. We can use it to determine the synthesized H_2O_2 concentration. 7.5 ml [$Ti(SO_4)_2$, 120 g/l] was added to 250 ml H_2SO_4 (1.5 M) to obtain the test solution of titanium sulfate. We used H_2O_2 with standard concentrations to obtain the proportionality between the absorption intensity of H_2O_2 at 410 nm, and the results are presented in Fig. S8(a). Once the proportionality is obtained, the H_2O_2 yield is estimated by the following equation:

$$C_{H_2O_2} = kIV \quad (4)$$

where k is the proportionality obtained by linearly fitting Fig. S8(b), I is the absorption intensity of synthesized H_2O_2 at 410 nm, and V is the solution volume (in our case, 400 ml).

Measurement of the pH value, conductivity, and temperature of the liquid. The pH value and temperature of the solution were measured by a pH detector with a temperature sensor (Yesmylab SX620), and the solution conductivity was measured by a conductivity detector (Yesmylab SX650).

Electrical characterization of the discharge plasma. The voltage between the tungsten steel and the graphite electrodes was measured by a high voltage (H.V.) probe (Tektronix P6015A) and the current was achieved from dividing the voltage across a 10- Ω resistor which was in series connected with the graphite electrode.

References

- Hill, C. A Vertical Empire: the History of the UK Rocket and Space Programme, 1950–1971. (World Scientific, 2001).
- Campos-Martin, J. M., Blanco-Brieva, G. & Fierro, J. L. Hydrogen peroxide synthesis: an outlook beyond the anthraquinone process. *Angew. Chem. Int. Ed.* **45**, 6962–6984 (2006).
- Centi, G., Perathoner, S. & Abate, S. in *Modern Heterogeneous Oxidation Catalysis: Design, Reactions and Characterization* 253–287 (2009).
- Landon, P., Collier, P. J., Papworth, A. J., Kiely, C. J. & Hutchings, G. J. Direct formation of hydrogen peroxide from H₂/O₂ using a gold catalyst. *Chem. Comm.*, 2058–2059 (2002).
- Nomura, Y. *et al.* Nanocolloidal Pd-Au as Catalyst for the Direct Synthesis of Hydrogen Peroxide from H₂ and O₂. *ChemSusChem* **1**, 619–621 (2008).
- Edwards, J. K. *et al.* The Direct Synthesis of Hydrogen Peroxide Using Platinum-Promoted Gold-Palladium Catalysts. *Angew. Chem. Int. Ed.* **53**, 2381–2384 (2014).
- Murayama, T. & Yamanaka, I. Electrosynthesis of neutral H₂O₂ solution from O₂ and water at a mixed carbon cathode using an exposed solid-polymer-electrolyte electrolysis cell. *J. Phys. Chem. C* **115**, 5792–5799 (2011).
- Yamanaka, I., Onizawa, T., Takenaka, S. & Otsuka, K. Direct and Continuous Production of Hydrogen Peroxide with 93% Selectivity Using a Fuel-Cell System. *Angew. Chem. Int. Ed.* **42**, 3653–3655 (2003).
- Murayama, T. & Yamanaka, I. Neutral H₂O₂ Synthesis by Electrolysis of O₂ and Water. *ECS Trans.* **25**, 19–24 (2010).
- Yamanaka, I. & Murayama, T. Neutral H₂O₂ synthesis by electrolysis of water and O₂. *Angew. Chem. Int. Ed.* **47**, 1900–1902 (2008).
- Liu, Y., Quan, X., Fan, X., Wang, H. & Chen, S. High-Yield Electrosynthesis of Hydrogen Peroxide from Oxygen Reduction by Hierarchically Porous Carbon. *Angew. Chem. Int. Ed.* **54**, 6837–6841 (2015).
- Cai, R., Hashimoto, K., Fujishima, A. & Kubota, Y. Conversion of photogenerated superoxide anion into hydrogen peroxide in TiO₂ suspension system. *J. Electroanal. Chem.* **326**, 345–350 (1992).
- Kormann, C., Bahnemann, D. W. & Hoffmann, M. R. Photocatalytic production of hydrogen peroxides and organic peroxides in aqueous suspensions of titanium dioxide, zinc oxide, and desert sand. *Environ. Sci. Technol.* **22**, 798–806 (1988).
- Cai, R., Kubota, Y. & Fujishima, A. Effect of copper ions on the formation of hydrogen peroxide from photocatalytic titanium dioxide particles. *J. Catal.* **219**, 214–218 (2003).
- Satterfield, C. N. & Bonnell, A. H. Interferences in titanium sulfate method for hydrogen peroxide. *Anal. Chem.* **27**, 1174–1175 (1955).
- Shiraishi, Y. *et al.* Sunlight-Driven Hydrogen Peroxide Production from Water and Molecular Oxygen by Metal-Free Photocatalysts. *Angew. Chem. Int. Ed.* **126**, 13672–13677 (2014).
- Venugopalan, M. & Jones, R. Chemistry of dissociated water vapor and related systems. *Chem. Rev.* **66**, 133–160 (1966).
- Morinaga, K. The Reaction of Hydrogen and Oxygen through a Silent Electric Discharge. I. The Formation of Hydrogen Peroxide. *Bull. Chem. Soc. Jpn.* **35**, 345–348 (1962).
- Yi, Y. *et al.* Safe direct synthesis of high purity H₂O₂ through a H₂/O₂ plasma reaction. *Angew. Chem. Int. Ed.* **52**, 8446–8449 (2013).
- Liu, Z. *et al.* Physicochemical processes in the indirect interaction between surface air plasma and deionized water. *J. Phys. D: Appl. Phys.* **48**, 495201 (2015).
- Chen, Q., Li, J. & Li, Y. A review of plasma-liquid interactions for nanomaterial synthesis. *J. Phys. D: Appl. Phys.* **48**, 424005 (2015).
- Mariotti, D., Patel, J., Švrček, V. & Maguire, P. Plasma-liquid interactions at atmospheric pressure for nanomaterials synthesis and surface engineering. *Plasma Process Polym.* **9**, 1074–1085 (2012).
- Akolkara, R. & Sankarana, R. M. Charge transfer processes at the interface between plasmas and liquids. *J. Vac. Sci. Technol. A* **31**, 050811 (2013).
- Richmonds, C. *et al.* Electron-Transfer Reactions at the Plasma-Liquid Interface. *J. Am. Chem. Soc.* **133**, 17582–17585 (2011).
- Rumbach, P., Bartels, D. M., Sankaran, R. M. & Go, D. B. The solvation of electrons by an atmospheric-pressure plasma. *Nat. Comm.* **6**, 8248 (2015).
- Bruggeman, P. & Schram, D. C. On OH production in water containing atmospheric pressure plasmas. *Plasma Sources Sci. Technol.* **19**, 045025 (2010).
- Bobkova, E., Shikova, T., Grinevich, V. & Rybkin, V. Mechanism of hydrogen peroxide formation in electrolytic-cathode atmospheric-pressure direct-current discharge. *High Energy Chem.* **46**, 56–59 (2012).
- Locke, B. R. & Shih, K.-Y. Review of the methods to form hydrogen peroxide in electrical discharge plasma with liquid water. *Plasma Sources Sci. Technol.* **20**, 034006 (2011).
- Lukeš, P. *Water treatment by pulsed streamer corona discharge* (2001).
- Burlica, R. & Locke, B. R. Pulsed plasma gliding-arc discharges with water spray. *IEEE Trans. Ind. Appl.* **44**, 482–489 (2008).
- De Baerdemaeker, F., Šimek, M., Člupek, M., Lukeš, P. & Leys, C. Hydrogen peroxide production in capillary underwater discharges. *Czechoslovak J. Phys.* **56**, B1132–B1139 (2006).
- Lukes, P., Appleton, A. T. & Locke, B. R. Hydrogen peroxide and ozone formation in hybrid gas-liquid electrical discharge reactors. *IEEE Trans. Ind. Appl.* **40**, 60–67 (2004).
- Lukes, P., Dolezalova, E., Sisrova, I. & Clupek, M. Aqueous-phase chemistry and bactericidal effects from an air discharge plasma in contact with water: evidence for the formation of peroxynitrite through a pseudo-second-order post-discharge reaction of H₂O₂ and HNO₂. *Plasma Sources Sci. Technol.* **23**, 015019 (2014).
- Hsieh, K. C., Wang, H. & Locke, B. R. Analysis of Electrical Discharge Plasma in a Gas-Liquid Flow Reactor Using Optical Emission Spectroscopy and the Formation of Hydrogen Peroxide. *Plasma Process Polym.* (2016).
- Thagard, S. M., Takashima, K. & Mizuno, A. Chemistry of the positive and negative electrical discharges formed in liquid water and above a gas-liquid surface. *Plasma Chem. Plasma Process* **29**, 455–473 (2009).
- Bruggeman, P. *et al.* Dc excited glow discharges in atmospheric pressure air in pin-to-water electrode systems. *J. Phys. D: Appl. Phys.* **41**, 215201 (2008).
- Chen, Q., Kaneko, T. & Hatakeyama, R. Reductants in gold nanoparticle synthesis using gas-liquid interfacial discharge plasmas. *Appl. Phys. Express* **5**, 086201 (2012).
- Cserfalvi, T. & Mezei, P. Direct solution analysis by glow discharge: electrolyte-cathode discharge spectrometry. *J. Anal. At. Spectrom.* **9**, 345–349 (1994).
- Chen, Q., Kaneko, T. & Hatakeyama, R. Rapid synthesis of water-soluble gold nanoparticles with control of size and assembly using gas-liquid interfacial discharge plasma. *Chem. Phys. Lett.* **521**, 113–117 (2012).
- Kaneko, T., Chen, Q., Harada, T. & Hatakeyama, R. Structural and reactive kinetics in gas-liquid interfacial plasmas. *Plasma Sources Sci. Technol.* **20**, 034014 (2011).
- Lieberman, M. A. & Lichtenberg, A. J. *Principles of Plasma Discharges and Materials Processing*. (John Wiley & Sons, 2005).
- Kebarle, P. A brief overview of the present status of the mechanisms involved in electrospray mass spectrometry. *J. Mass Spectrom.* **35**, 804–817 (2000).

43. Thomson, B. & Iribarne, J. Field induced ion evaporation from liquid surfaces at atmospheric pressure. *J. Chem. Phys.* **71**, 4451–4463 (1979).
44. Kebarle, P. & Tang, L. From ions in solution to ions in the gas phase—the mechanism of electrospray mass spectrometry. *Anal. Chem.* **65**, 972A–986A (1993).
45. Nicoll, W. & Smith, A. Stability of dilute alkaline solutions of hydrogen peroxide. *Ind. Eng. Chem.* **47**, 2548–2554 (1955).
46. Gurman, M., Shcherbak, L. & Rasskazov, A. Gold and arsenic recovery from calcinates of rebellious pyrite–arsenopyrite concentrates. *J. Min. Sci.* **51**, 586–590 (2015).
47. Chlistunoff, J. & Simonin, J.-P. Ionic association of hydroperoxide anion HO₂⁻ in the binding mean spherical approximation. Spectroscopic study of hydrogen peroxide in concentrated sodium hydroxide solutions. *J. Phys. Chem. A* **110**, 13868–13876 (2006).
48. Alshammari, Y. & Hellgardt, K. Partial oxidation of n-hexadecane through decomposition of hydrogen peroxide in supercritical water. *Chem. Eng. Res. Des.* **93**, 565–575 (2015).
49. Dai, X. J. *et al.* Efficient and Selectable Production of Reactive Species Using a Nanosecond Pulsed Discharge in Gas Bubbles in Liquid. *Plasma Process Polym.* 306–310 (2015).
50. Eisenberg, G. Colorimetric Determination of Hydrogen Peroxide. *Ind. Eng. Chem.* **15**, 327–328, doi: 10.1021/i560117a011 (1943).

Acknowledgements

This work was partially supported by the National Natural Science Foundation of China (Grant Nos.: 11405144, 11275261, 11304132, 61376068), the Fundamental Research Funds for the Central Universities (Grant Nos: 20720150022, 20720150083), the Natural Science Foundation of Fujian Province (2014J01025), and the Natural Science Foundation of Guangdong Province (Grant No. 2015A030313005). One of the authors Q. X. gives thanks for the funding supports by National Natural Science Foundation of China (Grant No: 11305273), and the Fundamental Research Funds for the Central Universities (Grant No: 0213005202054).

Author Contributions

Q.C. designed the experiments and supervised the project. J.L. and B.H. conducted the experiments, all the data analysis and interpretation guided by Q.C. and H.L. J.L., Q.X., G.Y., X.Z., S.Y. and Q.H.L. provided valuable discussions on the purpose and focus of the study. All authors discussed the results and Q.C. wrote the manuscript.

Additional Information

Supplementary information accompanies this paper at <http://www.nature.com/srep>

Competing financial interests: The authors declare no competing financial interests.

How to cite this article: Liu, J. *et al.* Direct synthesis of hydrogen peroxide from plasma-water interactions. *Sci. Rep.* **6**, 38454; doi: 10.1038/srep38454 (2016).

Publisher's note: Springer Nature remains neutral with regard to jurisdictional claims in published maps and institutional affiliations.



This work is licensed under a Creative Commons Attribution 4.0 International License. The images or other third party material in this article are included in the article's Creative Commons license, unless indicated otherwise in the credit line; if the material is not included under the Creative Commons license, users will need to obtain permission from the license holder to reproduce the material. To view a copy of this license, visit <http://creativecommons.org/licenses/by/4.0/>

© The Author(s) 2016